CuO-TiO$_2$ as a visible light responsive photocatalyst for the photoelectroreduction of CO$_2$ to methanol

Kaykobad Md. Rezaul Karim[1], Mariotte Anak Patrick Jebi[1], Huei Ruey Ong[2], Hamidah Abdullah[1,] Mostafa Tarek [1], Chin Kui Cheng[1], Md. Maksudur Rahman Khan[1,3]*

[1]Faculty of Chemical and Natural Resources Engineering, Universiti Malaysia Pahang, Lebuhraya Tun Razak, 26300 Kuantan, Pahang, Malaysia.
[2]Faculty of Engineering and Technology, DRB-HICOM University of Automotive Malaysia, 26607 Pekan, Pahang, Malaysia.
[3]Centre of Excellence for Advanced Research in Fluid Flow (CARIFF), University Malaysia Pahang, 26300 Kuantan, Pahang, Malaysia.
*E-mail: mrkhancep@yahoo.com, Tel. +6095492872, fax: +6095492889

Abstract - As rising atmospheric CO$_2$ levels change Earth's climate change, CO$_2$ reduction has become an increasingly active area in energy research over the past several years. The present work is developing artificial photosynthesis technologies that use visible light to convert CO$_2$ and water into methanol. In this study, TiO$_2$ loaded copper oxide (CuO-TiO$_2$)   was synthesized, characterized and studied for photoelectrochemical (PEC) reduction of CO$_2$ into methanol under visible light ($\lambda > 470$ nm) irradiation. In this perspective, the catalyst was synthesized via Sol-gel method. Catalyst characterization was done by X-ray diffraction (XRD), X-ray photoelectron spectroscopy (XPS), UV-vis absorption spectra, and Mott-Schottky (MS). Linear sweep voltammetry (LSV) was employed to evaluate the photocatalytic activity of the prepared photocatalyst under visible light ($\lambda > 420$ nm) irradiation for CO$_2$ reduction reactions. XRD results indicated that the particle size of the as-prepared photocatalyst was 65 nm. The oxidation state of Cu^{2+} and Ti^{4+} were confirmed by XPS results.   The band gap of CuO-TiO$_2$ composite characterization results indicated that the band gap energy of the CuO-TiO$_2$ catalyst was 1.68 eV. The flat band potential was calculated from the MS data and was found at 0.83 V vs NHE. During LSV, the onset potential was shifted positively (~100 mV) under the light on condition than the dark condition in CO$_2$ saturated solution suggests an increase in photocurrent and occurrence CO$_2$ photoreduction reaction.   The PEC performance of CuO-TiO$_2$ photocatalyst showed an increased methanol formation and found the optimum yield of 20.1 μmol.L^{-1}cm^{-2} under visible light irradiation.

Keywords: CO$_2$ reduction; Photoelectrochemical; visible light; CuO-TiO$_2$ photocathode; methanol

1. INTRODUCTION

The rapid emissions of CO2 in atmospheric possed one of the most crucial issues with regard to the greenhouse effect. This issue has raised multiple concerns to find different CO2 mitigation technologies and strategies into a clean energy fuel. The mimic photosynthesis process has sparked a new sustainable development way in recent years in order to solve major issues nowadays: climate change and energy shortage, which can be implemented using water (H$_2$O) as both proton and electron supply photoreduction of H$_2$O and CO$_2$ into hydrocarbons fuels [1] The idea of converting CO$_2$ to hydrocarbons is originates from natural photosynthesis process which produce carbohydrate and oxygen from H$_2$O and CO$_2$, via the harvest and exploitation of solar energy. However, since CO$_2$ is chemically stable, the conversion of CO$_2$ is quite difficult without the assistance of any catalyst and requires large energy input [2]. In this research area, solar photocatalytic reduction of CO$_2$ has been extensively investigated. Generally, photocatalysis (PC) requires photoresponsive materials capable of harvesting solar light to produce photogenerated electrons and enable to transfer multiple electrons for the formation of different products. Although photocatalysis is the most promising solutions but typically suffers from mechanistic complexity, poor product selectivity and slow kinetics[3]. The one electron reduction of CO$_2$ to generate CO$_2^-$ is not easily possible because in the reduction of CO$_2$ the first electron transfer to generate CO$_2^-$ requires nearly -1.90 V vs NHE and it is an uphill process with great over potential. Thus, a novel light-driven and electrically biased PEC cell as the combination of electrocatalysis and photocatalysis is one of the key improvement to overcome the low product selectivity and reduce energy input over photocatalyst (Li, et al., 2015).

Toward this artificial photosynthesis, the photocatalyst is typically a hybrid material capable of produce photogenerated electrons by absorbs visible light. The photogenerated electrons are separated and reached in the catalyst surface and offer active sites for further catalytic reaction. [4]. TiO_2 is one of the optimistic photocatalysts due to its excellent properties, such as high stability, non-toxicity and low cost and [5]. However, it was known that TiO_2 (band gap 3.2 eV) is a UV light-driven photocatalyst limited to a high e^-/h^+ recombination rate [6]. On the other hand, semiconductors suffer from low quantum efficiencies and selectivity due to the formation of H_2 in an aqueous solution simultaneously during CO_2 reduction. H_2 formation reaction is the main competitive reaction which should be suppressed to produce a selective product during the CO_2 reaction. Artificial photosynthesis could be achieved by using an appropriate photocathode for CO_2 reduction. In order to solve low quantum yield and selectivity problems, multiple attempts on band gap tuning to make TiO_2 active for visible light photocatalyst by introducing defects with transition metals. In CO_2 reduction, the addition of TiO_2 cocatalysts has been investigated including RGO–Cu_2O [7], N_2doped TiO_2 [8] and $Cu_xO−TiO_2$ [9]. Thus, helped to improve electron-hole separation and act as sink onto photocatalyst surface and to improve the photocatalytic efficiency. At hybrid $CuxO-TiO_2$ heterostructured composite a remarkable methane formation was observed during CO_2 reduction and found as 221.63 ppm $g^{-1}h^{-1}$. The photocatalytic CO_2 reduction efficiency of Cu_2O can be improved by coupling Cu_2O with TiO_2, acting as a charge transfer enhancing layer [9].

To the best of our understanding, so far there was no information in the literature on $CuO-TiO_2$ catalyst for photoelectroreduction of CO_2 to liquid products under visible light irradiation. Another approach is to couple TiO_2 to CuO, a p-type semiconductor can exist in different stoichiometry and phases such as Cu_2O and CuO with narrow band gap energy from 1.2 to 2 e.V. The band gap energy (Eg = 1.35–1.7 eV) of CuO lies near the CO_2/O_2 potential and are used as a visible light active photocatalyst [10]. Thus, $CuO-TiO_2$ represent one of the most appealing systems and is expected to produce an enhanced charge carrier lifetime, with beneficial impact both on catalytic performance [11]. Therefore, this study is to synthesise and characterizes $CuO-TiO_2$ as a visible light responsive photocatalyst that used in CO_2 photoelectrochemical reduction into methanol under solar light irradiation. The catalyst was characterized by using UV-Vis, XRD and XPS. The photoelectrochemical behaviour of the catalyst for CO_2 reduction was evaluated by LSV and MS analysis.

2. EXPERIMENTAL

A. Materials and Methods

Copper (II) nitrate trihydrate, Cu(NO3)2.3H2O (99%) (2.3 g), titanium (IV) dioxide, TiO2 (99%) (2.53 g), hydrazine monohydrate, N2H4. H2O (0.347 M), ascorbic acid and NaHCO3 are of the analytical condition and used without extra purification.

B. Preparation of CuO-TiO2

The $CuO-TiO_2$ was prepared by Sol-gel method. A required amount of $Cu(NO_3)_{2.3}H_2O$ and TiO_2 Degussa-P25 powder, and ascorbic acid (0.02M) were dispersed into the solution of 50 ml distilled water. After that, 11 mL of $N_2H_4 \cdot H_2O$ (0.347 M) act as reducing agent was added into the reaction mixture with continuous stirring at room temperature for ~ 4 h until colour changes from blue to red precipitate (Ramli, et al., 2014). The paste sample was then dried at 70°C, 0.5 MPa in a vacuum oven for overnight. Finally, the sample was grinded into a fine powder using marble mortar.

The electrodes were prepared with the method described by Woon et al., Ong et al. [12], [13]. Briefly, the catalyst ink was prepared by mixing 22 mg of $CuO-TiO_2$ with 140 µL of 5 wt% Nafion and 280 µL isopropanol (C_3H_8O) followed by ultrasonication for 30 min. Thereafter, the ink was evenly brushed with an area of 1 cm^2 of graphite paper. The electrode was dried in vacuum oven at 90 °C for 6 h.

C. Catalyst characterization

X-ray diffraction (XRD was performed by Rigaku Mini Flex II (30 kV and 15 mA), Japan to determine the broadening of the diffraction peak of the prepared catalysts. The specimens will be step-wise scanned over the operational range of scattering angle (2θ) between 10° to 80°, with a scan step of 0.02°/min. The data were recorded in terms of the diffracted X-ray intensity (I) versus 2θ. Ultraviolet-visible (UV-NIR) absorption spectroscopy was conducted by Shimadzu UV-2600. XPS study was performed using a VG Microtech MT500 with an Mg-Kα X-ray source. MS experiment was done at 2000 Hz frequencies by using an electrochemical analyser (Autolab Compact PGSTAT 204, Netherland) with an Ag/AgCl electrode, $CuO-TiO_2$

electrode and platinum foil used as a reference electrode, working electrode and counter electrode respectively in 0.1 M $NaHCO_3$ aqueous solution (pH 6.8)

D. *Photoelectrochemical measurement*

All PEC reduction of the CO_2 study were performed in a single chamber PEC cell equipped with a quartz window reactor as illustrated in Figure 1. All the PEC measurement were completed by using a potentiostat (Autolab Compact PGSTAT 204, Netherland) using a typical three electrode-system consists of Ag/AgCl electrode, CuO-TiO_2 electrode and platinum foil used as a reference electrode, working electrode and counter electrode respectively in 0.1 M $NaHCO_3$ aqueous solution (pH 6.8) Prior to start the reaction, high purity CO_2 (99.99%) gas was purged in to the 0.1M $NaHCO_3$ aqueous solution for 30 min at a fixed flow rate so that the concentration of CO_2 into the solution reached saturation. LSV was carried out from the potential range of -0.2 to -0.8 V vs NHE with 10 mV/s scan rate. Light irradiation (Light source: XD-300 High Brightness Cold Light Source, Beijing Perfect light Co., Ltd., China,) was kept constant during LSV scanning light on the condition.
For product analysis, 5 mL of aqueous reaction sample was withdrawn at a different time interval and was quantified by DB-WAX 123-7033 column (30 m x 0.32 mm x 0.5μm) in GC-FID equipped with 7694 E headspace autosampler injection for methanol (CH_3OH) analysis.
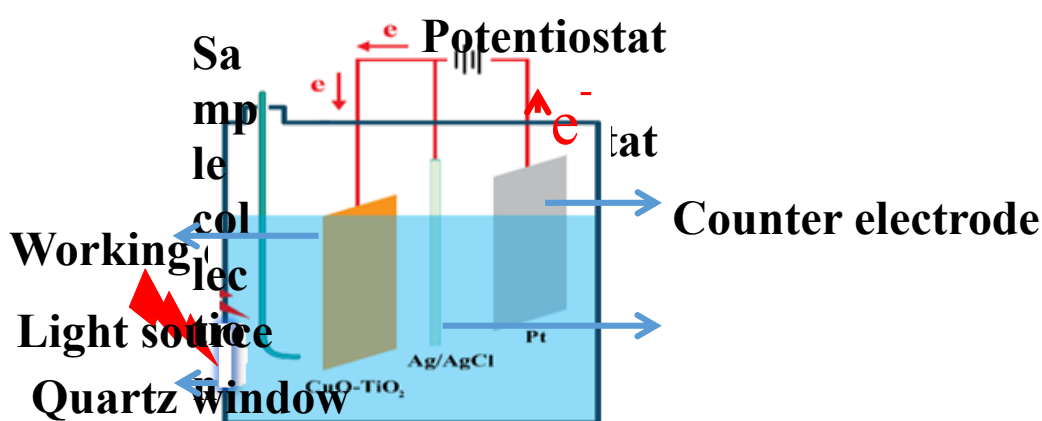

Figure1: Schematic diagram of PEC reduction of CO_2 on CuO-TiO_2

3. RESULTS AND DISCUSSION

A. *Characterization of CuO-TiO2*

Figure 2(a) depicted the absorbance chart for wavelength 200 to 900 nm which shows the visible light response capacity of the prepared photocatalysts. The band gap of the as-prepared catalysts was determined by using the tauc plot as shown in Figure 2 (b) which represents the indirect transition of band gap energy values by plotting $(\alpha h\upsilon)^{1/2}$ versus $h\upsilon$. The band gap of the commercial TiO_2 was found 3.3 eV which correspond to wavelength absorption of 397 nm and the CuO-TiO_2 with a higher intensity of absorption displayed lower optical band gap energy of 1.68 eV as expected for CuO according to literature reports [14]. When a metal or compound is loaded to the other catalyst, the previous band gap may be shifted to a new band gap. Commercial TiO_2 can be used as an effective bandgap modifier to absorb the light ranging under the visible light region [9]. Therefore, the as-prepared CuO-TiO_2 composite catalysts with low band gap can be able to enhance the photoabsorption capacity towards the visible light region.
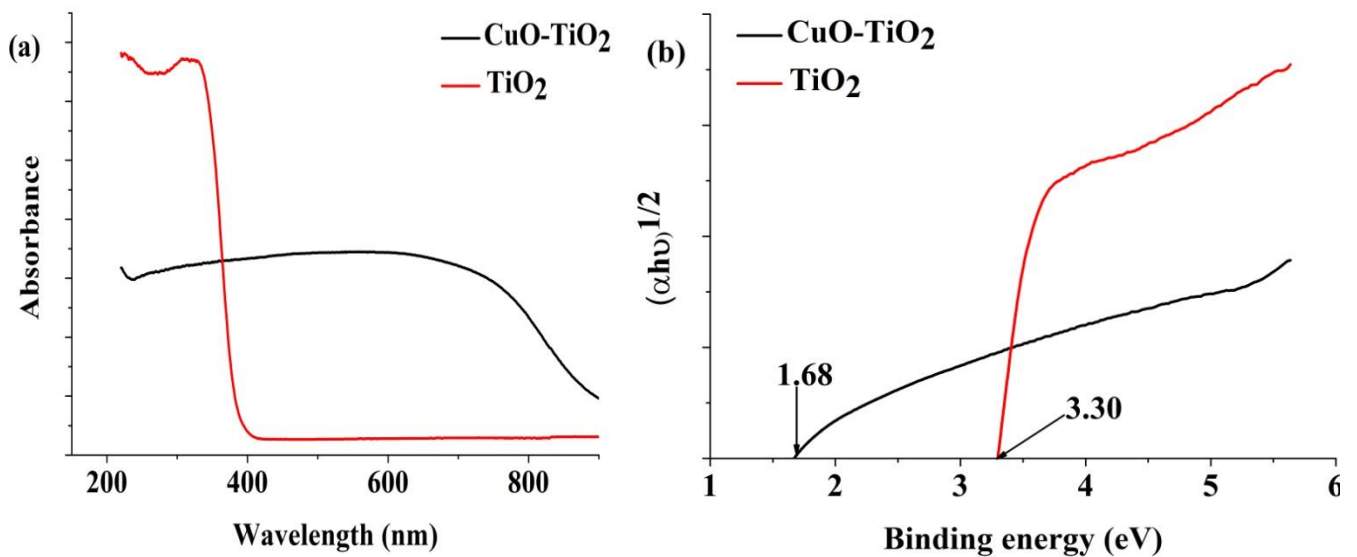
Figure 2: (a) UV-Vis spectrum of CuO-TiO₂ (b) Tauc plot for band gap energy calculation of as-prepared photocatalysts.

Figure 3 shows the XRD pattern of the as-prepared CuO-TiO$_2$. From the JCPDS Card No. 45-937 database, all the diffraction peak position of can be indexed as monoclinic CuO phase (Barreca, et al., 2011). In particular, the patterns showed the reflections peaks on 2θ = 32.44°, 38.72°, 48.7°, 53.40°, 58.25°, 66.20°, 72.4°, and 75.2 can be easily indexed to (110), (111), (202), (320), (321), (410), (511) and (622) crystal planes, respectively (JCPDS Card No. 45-937) with lattice parameters a_0 = 4.684, b_0 = 3.425 and c_0 = 5.129 Å. The peaks matching well with the anatase TiO$_2$, the relative peak around at 35.09°, 61.61°, and 67.48° are indexed to the diffraction of the (311), (422) and (611) plane of the TiO$_2$ indicating that TiO$_2$ and CuO coexist in the CuO-TiO$_2$ heterojunction. This is understandable because the lattice constants of anatase TiO$_2$ are similar to those of CuO [15] Therefore, from diffraction pattern it can be concluded that crystalline CuO on TiO$_2$ has been formed.
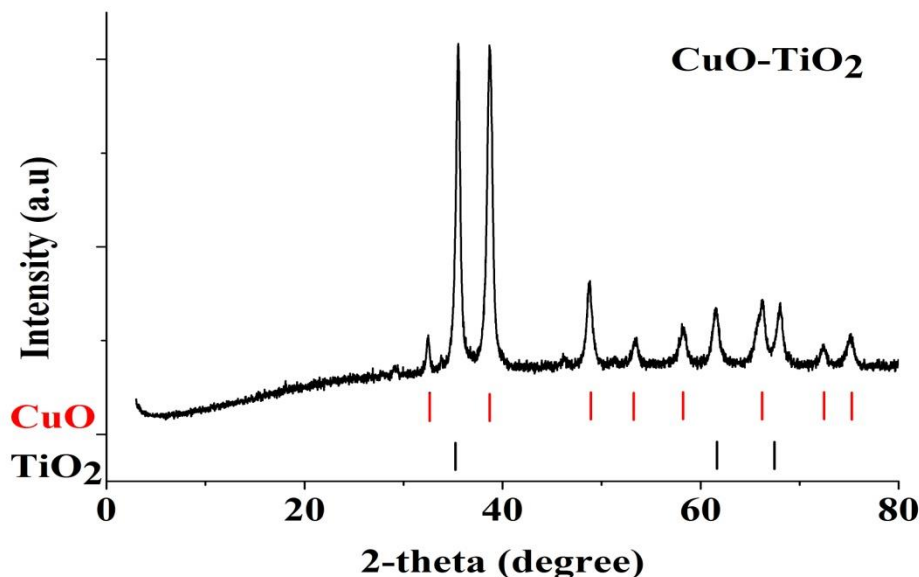

Figure 3: XRD patterns on the as-prepared CuO-TiO₂

 XPS was done to identify the oxidation state of Cu and Ti on CuO-TiO$_2$ composite catalyst. The XPS spectra of Cu2p   Figure 4(a) demonstrate the existence of Cu2p1/2 (binding energy at 951.9 eV) and Cu2p3/2 (binding energy at 932.2 eV). Furthermore, shake-up peak at 942.8 eV and 940.6 eV are indicative of the presence of Cu^{2+} in the composite catalyst. The XPS spectra of   Ti in Figure 4 (b) shows three peaks at 461.5 eV, 456.09 eV and 452.2 eV. The first peak is assigned for Ti2p1/2 whereas the other two peaks are assigned for for Ti2p3/2 (Park, et al., 2016). The o 1s spectrum shown in figure 4(c) shows a major peak at 530.0 eV matches to O^{2-} in CuO and TiO$_2$ and a secondary peak at 531.0 eV is assigned to the oxygen species adsorbed on the surface [16].
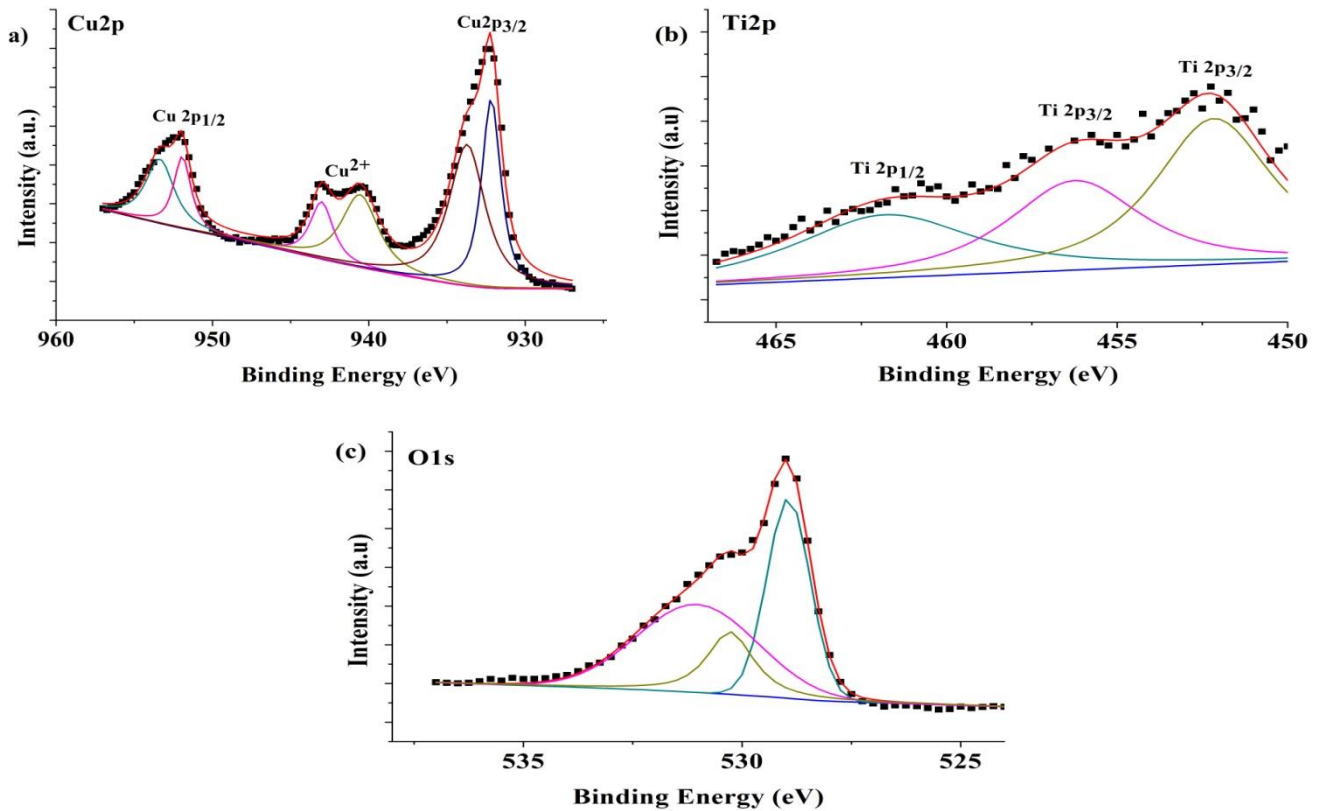
Figure 4: XPS spectra for (a) Cu2p and (b) Ti2p and (c)O 1s in CuO-TiO$_2$

To find out the valence band position of the prepared catalyst, the Mott-Schottky analysis was carried out in 0.1 M NaHCO$_3$ solutions (pH 6.8) shown in Figure 5 (a). Flat band potential (E$_{fb}$) is normally situated close to the VB, and it can be calculated from the intersection of a plot of $1/C^2$ against E by the following equation 1 [17]:

$$\frac{1}{C^2} = \frac{2}{e \in \in_0 N} \left(E\text{-}E_{fb}\text{-}\frac{kT}{e} \right) \ldots \ldots \ldots \ldots \ldots \ldots \ldots \ldots \ldots . . (1)$$

where C, e, $\in$, $\in_0$ are the capacitance, electron charge, dielectric constant and permittivity of vacuum respectively, whereas the N, E, E$_{fb,}$ k and T are the acceptor density, electrode potential, flat band potential, Boltzmann constant, and temperature respectively. Figure 5a shows that the x-axis intercept was 0.80 V vs NHE. The flat band potential was calculated using the equation (1) and found e 0.83 V vs NHE. Figure 5b displays the band diagram for CuO-TiO$_2$ and the thermodynamic redox potential of CO$_2$ reduction (V vs NHE). The calculated VB and CB potential of CuO-TiO$_2$ were approximately -0.83 and -0.85 V versus an NHE, respectively. Due to a higher CB of CuO-TiO$_2$ than that of the redox potential of CO$_2$, the excited electrons in the CB can be easily used by the CO$_2$ molecules and converted toits reduced products. Moreover, with the assistance of an external bias potential electron-hole recombination rate will be low leading to the efficient photoelectrochemical reduction of CO$_2$ [18].
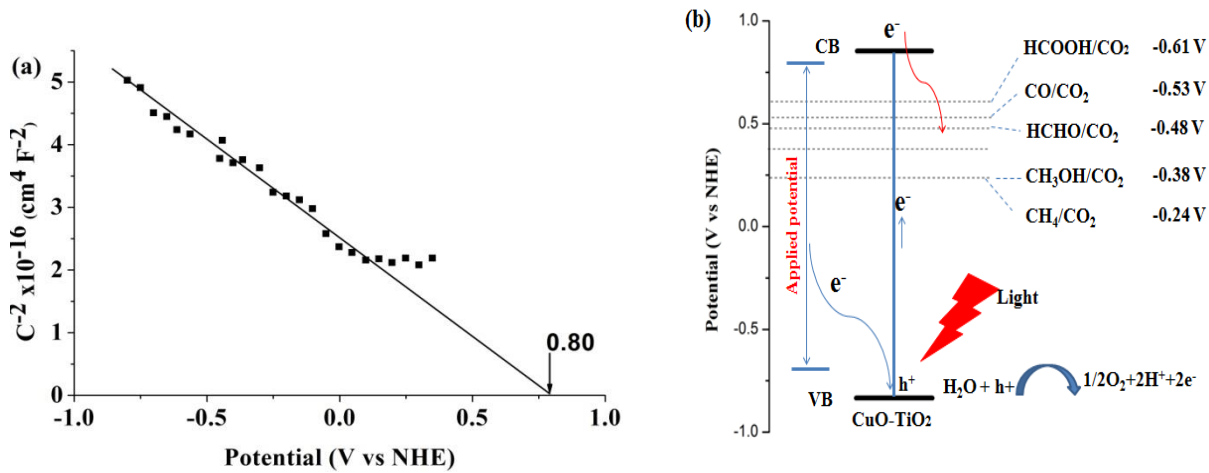
Figure 5: (a) Mott-Schottky plot of CuO-TiO$_2$ at 2000 Hz   (b) Position of the conduction band and valence band of CuO-TiO$_2$ photocathode together with the redox potential of various reduction products at pH 6.8.

B.   Photoelectrochemical performance

Figure 6 depicted the LSV for CuO-TiO$_2$ in 0.1M NaHCO$_3$ solution with the N$_2$-saturated and CO$_2$-saturated solution under dark and visible light illumination at scan rate 10 mV/s. Higher reduction photocurrent under CO$_2$- saturated than under a N$_2$-saturated environment was observed, indicating the CO$_2$ reducibility of CuO-TiO$_2$ under the light on condition.. The cathodic current was increased as the applied potential increased for light on compared to light off condition. This phenomenon might be due to water/proton reduction [19].   In contrast, it was observed that with light irradiation, the cathodic current profile for CuO-TiO$_2$ was improved with the copper loading with onset potential value from -0.2V with maximum current at -0.8V versus NHE. A remarkable shift of onset potential to the positive region, indicating the reaction could occur with less applied potential in presence of light.
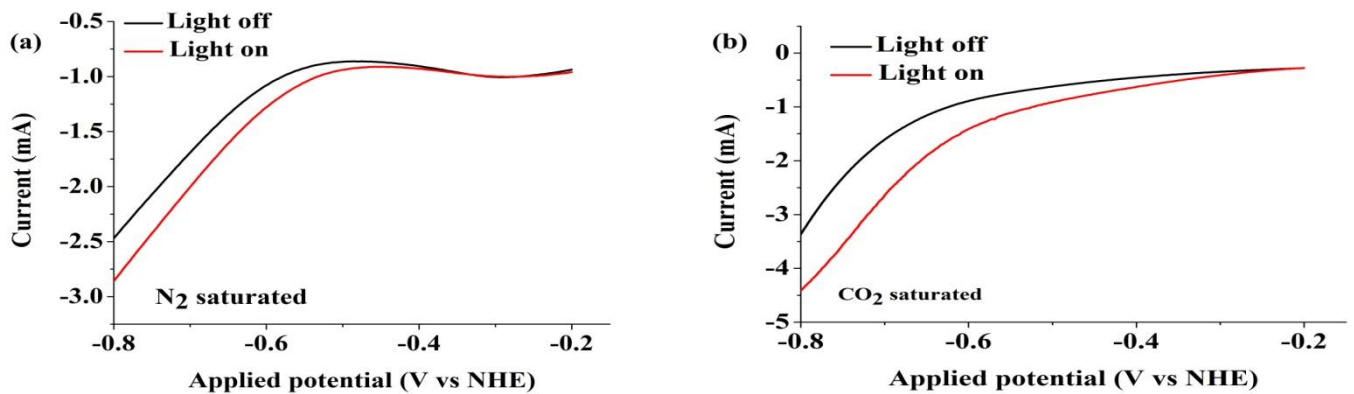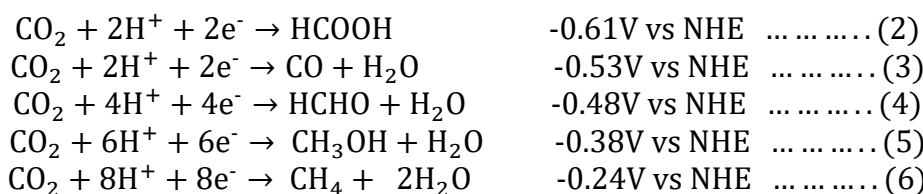

Figure 6: LSV of CuO-TiO$_2$ electrode N$_2$-saturated and CO$_2$-saturated 0.1 M NaHCO$_3$ solution under light on/off (scan rate 10 mV/s; light wavelength = 470 nm)

Proton-coupled multiple electron reduction reactions may occur over CuO-TiO$_2$ during CO$_2$ followed 2e$^-$, 4e$^-$, 6e$^-$ and 8e$^-$ pathway [20] can be described in Eqs. (2-6):

$$CO_2 + 2H^+ + 2e^- \rightarrow HCOOH \qquad \text{-0.61V vs NHE} \quad ……….. (2)$$
$$CO_2 + 2H^+ + 2e^- \rightarrow CO + H_2O \qquad \text{-0.53V vs NHE} \quad ……….. (3)$$
$$CO_2 + 4H^+ + 4e^- \rightarrow HCHO + H_2O \qquad \text{-0.48V vs NHE} \quad ……….. (4)$$
$$CO_2 + 6H^+ + 6e^- \rightarrow CH_3OH + H_2O \qquad \text{-0.38V vs NHE} \quad ……….. (5)$$
$$CO_2 + 8H^+ + 8e^- \rightarrow CH_4 + 2H_2O \qquad \text{-0.24V vs NHE} \quad ……….. (6)$$

The PEC, EC and PC reduction of CO_2 were conducted in 250 ml of CO_2-saturated 0.1 M $NaHCO_3$ solution at -0.36 V vs NHE under 470 nm wavelength irradiation for 4 hr (Figure7). In this work, methanol was found as the main product in the liquid phase as analysed in GC-FID. It was found out that during the blank experiment (only 0.1M $NaHCO_3$ solution without CO_2 purging), no other C1 products obtained, proving that carbon in CH_3OH originated from the purged CO_2. With CuO-TiO_2 electrode, the methanol yield increased as irradiation time progressed. At 4 h reaction time, amount of methanol yield for PC, EC and PEC was monitored to be 2.35, 15.40 and 20.1 $\mu mol.L^{-1}cm^{-2}$ respectively. Moreover, the resulting methanol yield in PEC system was better compared to the summation of EC and PC (17.75 $\mu mol.L^{-1}.cm^{-2}$) processes on CuO-TiO_2 confirming the synergistic effect in term of product yield.
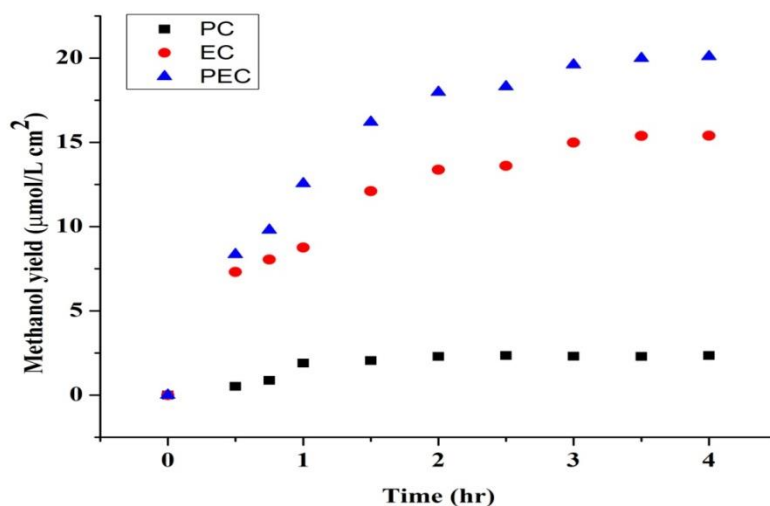

Figure7: Methanol yields under photoelectrocatalytic (PEC), electrocatalytic (EC) and photocatalytic (PC) conditions with reaction time over CuO-TiO_2 electrode.

Based on the above results, a possible mechanism was proposed for the PEC reduction of CO_2 to methanol in figure 8. Within the $CuO-TiO_2$ photocatalyst, the electrons (e^-) and holes (h^+) recombination process were inhibited by applying external bias potential. Upon light driven, photoelectrons generated from $CuO-TiO_2$ at VB jumps to CB, and promote the flows to CO_2 due to the band bending between the interface of the photocatalyst. To activate the inert CO_2 molecule for reduction, the best way is to absorb it on the surface of CuO-TiO_2 catalyst electrode. If a high-dielectric-constant solvent is used such as water, the CO_2^- anion radicals can be greatly stabilized by the solvent, resulting in weak interactions with the photocatalyst surface. After the adsorption, upon visible light irradiation, electrons and holes are produced and reaction initiates. Electron reached to the adsorbed CO_2 and reduced it to an anion radical $^{\cdot}CO_2^-$ whereas, H_2O oxidation proceeds through the holes, which make H^+, O_2 and excited electrons, which is being participated in the reaction. The H^+ further takes electrons and form $^{\cdot}H$, which reacts with the $^{\cdot}CO_2^{\ -}$ to make CO and OH^-.
 The CB of $CuO-TiO_2$ was -0.77 V vs NHE which was more negative than the reduction potential of CO_2/CH_3OH (-0.38 V vs. NHE), indicating that the prepared catalyst has enough PC to reduce CO_2 to CH_3OH. Besides this, the externally applied bias potential could not only improve the parting of electrons and holes to improve the CO2 reduction capacity but also supplied additional electrons to keep up the EC reduction of CO_2. However, the efficiency of the reaction could be low, due to the electron-hole (e-/h+) recombination process. Therefore, at minimum potentials of -0.36 V vs NHE, can assist CO_2 reduction and is important for selective product production. The PEC result was compared with   EC and PC system possesses two advantages: (i) the applied bias potential not only assists selective reaction but also enhances the partition of photoinduced charge carriers, enhancing PEC process; (ii) Visible light irradiation lowers the required potential for CO_2 reduction and promotes the electrode kinetics for a selective product, favouring the EC process thus capable to reduce CO_2 to CH_3OH [21].
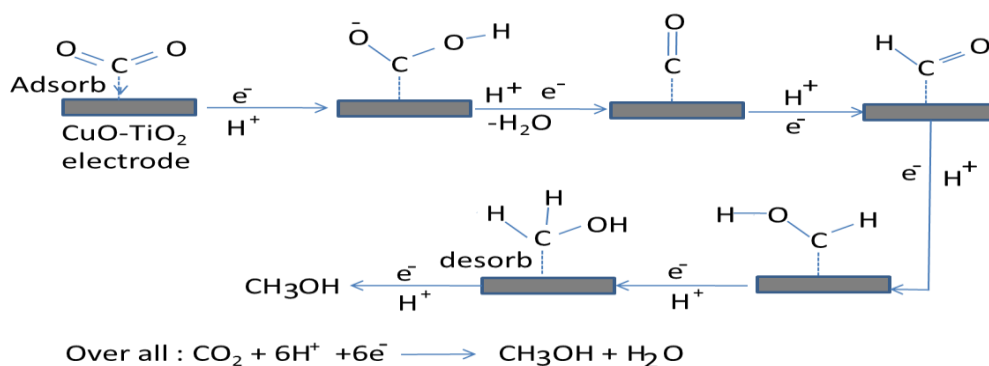
Figure 8: Scheme of CO_2 photoreduction mechanism on $CuO-TiO_2$ catalyst

4. CONCLUSION

The photoelectrocatalytic reduction of CO_2 in an aqueous solution under visible light irradiation was carried out successfully in the as-prepared $CuO-TiO_2$ composite catalyst prepared by Sol-gel method. The characterization results showed that the loading of CuO on TiO_2 reduced the band gap thus increased visible light absorption by shifting the bang-gap of commercial TiO_2 (3.3 eV) into a new band gap of $CuO-TiO_2$ (1.68 eV). The VB and CB position of $CuO-TiO_2$ was -0.83 V and -0.85 V versus a NHE, respectively that calculated from UV-Vis and Mott-Schottky result. Methanol yield in PEC system was found higher (20.1 $\mu mol.L^{-1}.cm^{-2}$) then PC and EC reaction system over $CuO-TiO_2$. The higher yield of methanol in PEC may be occurred due to the synergistic effect. An electron flow scheme was proposed to demonstrate the possible CO_2 reduction reaction. The separation of photo-induced carrier and hole was more effective under applied bias potential, and it enabled more photoelectrons availability at the surface CO_2 reduction active sites. Thus, further research is required to explore the effect of CuO loading on TiO_2 and mechanism phenomena for CO_2 reduction by PEC and understand the CO_2 reduction mechanism in depth.

REFERENCES

[1] T. Arai, et al., "Selective CO2 conversion to formate in water using a CZTS photocathode modified with a ruthenium complex polymer," Chemical Communications. 2011. **47**(47): p. 12664-12666.

[2] A. Sarkar, et al., "Photocatalytic reduction of CO2 with H2O over modified TiO2 nanofibers: Understanding the reduction pathway," Nano Research. 2016. **9**(7): p. 1956-1968.

[3] W. Tu, Y. Zhou, Z. Zou, "Photocatalytic Conversion of CO2 into Renewable Hydrocarbon Fuels: State-of-the-Art Accomplishment, Challenges, and Prospects," Advanced Materials. 2014. **26**(27): p. 4607-4626.

[4] J. Jiao, et al., "Photocatalysts of 3D Ordered Macroporous TiO2-Supported CeO2 Nanolayers: Design, Preparation, and Their Catalytic Performances for the Reduction of CO2 with H2O under Simulated Solar Irradiation," Industrial & Engineering Chemistry Research. 2014. **53**(44): p. 17345-17354.

[5] S. A. Ansari, et al., "Gold nanoparticles-sensitized wide and narrow band gap TiO2 for visible light applications: a comparative study," New Journal of Chemistry. 2015. **39**(6): p. 4708-4715.

[6] B. Fang, et al., "Hierarchical CuO–TiO2 Hollow Microspheres for Highly Efficient Photodriven Reduction of CO2 to CH4," ACS Sustainable Chemistry & Engineering. 2015. **3**(10): p. 2381-2388.

[7] X. An, K. Li, J. Tang, "Cu2O/Reduced Graphene Oxide Composites for the Photocatalytic Conversion of CO2," ChemSusChem. 2014. **7**(4): p. 1086-1093.

[8] M. S. Akple, et al., "Nitrogen-doped TiO2 microsheets with enhanced visible light photocatalytic activity for CO2 reduction," Chinese Journal of Catalysis. 2015. **36**(12): p. 2127-2134.

[9] S. M. Park, et al., "Hybrid CuxO–TiO2 Heterostructured Composites for Photocatalytic CO2 Reduction into Methane Using Solar Irradiation: Sunlight into Fuel," ACS Omega. 2016. **1**(5): p. 868-875.

[10] S. I. In, D. D. Vaughn, R. E. Schaak, "Hybrid CuO-TiO2−xNx Hollow Nanocubes for Photocatalytic Conversion of CO2 into Methane under Solar Irradiation," Angewandte Chemie International Edition. 2012. **51**(16): p. 3915-3918.

[11] D. Barreca, et al., "Novel Synthesis and Gas Sensing Performances of CuO–TiO2 Nanocomposites Functionalized with Au Nanoparticles," The Journal of Physical Chemistry C. 2011. **115**(21): p. 10510-10517.

[12] C. W. Woon, et al., "MnO2/CNT as ORR Electrocatalyst in Air-Cathode Microbial Fuel Cells," Procedia Chemistry. 2015. **16**: p. 640-647.

[13] M. R. Khan, et al., "Nanostructured Pt/MnO2 Catalysts and Their Performance for Oxygen Reduction Reaction in Air Cathode Microbial Fuel Cell," International Journal of Electrical, Computer, Electronics and Communication Engineering. 2015. **9**(3): p. 247–253.

[14] S. J. A. Moniz, J. Tang, "Charge Transfer and Photocatalytic Activity in CuO/TiO2 Nanoparticle Heterojunctions Synthesised through a Rapid, One-Pot, Microwave Solvothermal Route," ChemCatChem. 2015. **7**(11): p. 1659-1667.

[15] N. Thi Hiep, et al., "Synthesis and characterization of nano-CuO and CuO/TiO 2 photocatalysts. Advances in Natural Sciences," Nanoscience and Nanotechnology. 2013. **4**(2): p. 025002.

[16] Z. Jin, et al., "Photo-reduced Cu/CuO nanoclusters on TiO2 nanotube arrays as highly efficient and reusable catalyst," 2017. **7**: p. 39695.

[17] S. Kamimura, et al., "Fabrication and characterization of a p-type Cu 3 Nb 2 O 8 photocathode toward photoelectrochemical reduction of carbon dioxide," Applied Catalysis B: Environmental. 2015. **174**: p. 471-476.

[18] J. Gu, et al., "Mg-Doped CuFeO2 photocathodes for photoelectrochemical reduction of carbon dioxide," The Journal of Physical Chemistry C. 2013. **117**(24): p. 12415-12422.

[19] Q. Shen, et al., "High-yield and selective photoelectrocatalytic reduction of CO2 to formate by metallic copper decorated Co3O4 nanotube arrays," Environmental science & technology. 2015. **49**(9): p. 5828-5835.

[20] E. E. Benson, et al., "Electrocatalytic and homogeneous approaches to conversion of CO2 to liquid fuels," Chemical Society Reviews. 2009. **38**(1): p. 89-99.

[21] X. Huang, et al., "Synergistic Photoelectrochemical Synthesis of Formate from CO2 on {12$\bar{1}$} Hierarchical Co3O4," The Journal of Physical Chemistry C. 2013. **117**(50): p. 26432-26440.